2023 International Conference on Science, Engineering and Business for Sustainable Development Goals (SEB-SDG) | 979-8-3503-2478-5/23/$31.00 ©2023 IEEE | DOI: 10.1109/SEB-SDG57117.2023.10124471

Numerical Modeling and Investigation of Flow of Incompressible Non-Newtonian Fluids through Uniform Slightly Deformable Channel

Oluwaseyi O. **Alabi**
Department of Mechanical Engineering
University of Ibadan
engrseyialabi@gmail.com

Oyetunde A. **Adeaga**
Department of Mechanical and Mechatronics Engineering
First Technical University Ibadan
oyeadeaga@tech-u.edu.ng

Sarah A. **Akintola**
Department of Petroleum Engineering
University of Ibadan
Sarah.akintola@ui.edu.ng

Abstract— Numerical investigations of peristaltic flow of three non-Newtonian viscous fluids arising within modelled gut were performed to show their thermal and hydrodynamic behaviour in the gut. A 3-D numerical model of the human intestine was derived using Autodesk Inventor 2017 and simulated using ANSYS FLUENT 16.0. Thyme and produced Ogi, Soymilk and Sobo are considered working fluids. The density and viscosity of the produced fluid were determined experimentally, while the density and viscosity of the digester were obtained from previous work. The results of the experiments carried out showed that the densities of the produced fluid supplements were; 1024 kg/m³, 920 kg/m³ and 800 kg/m³ for Ogi, soybean milk and sobo respectively; their equivalent viscosities were; 1.095 Pa.s, 0.95 Pa.s, and 0.316 Pa.s. From the results, it can be seen that the velocity behaviour of the four fluids is similar, as is the thermal behaviour. The results also showed that at inlet velocity of 0.005 m/s, Ogi had the largest pressure change of 25 Pa and a heat transfer of Nu=9, while sobo had the smallest heat transfer of Nu=9 among the three fluid supplements produced. Nu=5.

Keywords— flow rate non-Newtonian fluid, gut, numerical, simulation, peristaltic flow Introduction

I. INTRODUCTION

Fluids are substances that deforms continuously under an applied shear stress, or substances that cannot resist when contacted. The mechanical behaviour of physiological fluids can either be Newtonian or non-Newtonian. Newtonian fluids are fluids in which stress and angular deformation varies directly with one another while viscosity is the constant of proportionality. Such fluids include water, air, urine etc. While for non-Newtonian fluids, shear stress varies not with angular deformation and viscosity becomes function of some parameter but they do depend on shear stress, e.g blood, chyme and starch (Cengel and Ghajar, 2015).

Non-Newtonian fluids may be classified as viscoelastic, dilatant, and pseudo plastic fluids. Dilatant fluids are fluids whose apparent viscosity increases with decreasing shear strain rate, where pseudo plastic fluids are those, whose viscosity decreases with increase in shear strain rate (Cengel and Ghajar, 2015). Malik et al., (2016) suggested that chyme is pseudo plastic due to its hydrodynamic properties. Chyme gradually passes through the small intestine through a process of mixing of non-Newtonian fluids and continuous digestion and absorption.

Imam et al., (2018) report that when a large bolus of food is swallowed, the peristaltic process begins in the oesophagus and continues in the small intestine, where it mixes and moves the chyme back and forth, allowing the supplement to be absorbed into the blood through wall of the small intestine. In humans, digestion of food begins in the mouth, where it is chewed and moistened by saliva, and then descends into the stomach through a peristaltic movement, this involves several forces and reactions that lead to three important motions within the gastrointestinal tract, which are the segmentation, peristalsis and pendular movements Adegun, Alabi, et al., (2020).

The knowledge of fluid flow in human intestines(small) is necessary to achieve good in vitro-in- vivo correlation to assess the effects of food formulation on the absorption profile of a supplement. According to Tharakan (2014), there are always enzyme-substrate interactions before food molecules are absorbed into the blood through the gut. This is the so-called bulk transfer of food nutrients through the intestinal wall into the body system. Thus, the hydrodynamics of chyme (digested food materials) in small intestine affects absorption profile due to fluid properties and transport mechanisms within human system. Blackburn et-al., (1984), reported the presence of 14.5 per 250 mL of glucose solution Keguar Gum during the delivery of fluid supplements to the intestinal wall due to the

convective mixing of intestinal contents known as chyme and its diffusion. Blackburn et-al., (1984), furthermore, asserted that food digestion involves two types of processes viz; mechanical and chemical digestion. The former is concerned with the motility processes towards facilitating the mixing and distribution of foods via the gastrointestinal (GI) tract while the latter is responsible for the catabolic lipids and towards breaking down of carbohydrates into small molecules so that it can easily absorbed by cell membranes.

Macagno and Christensen, 1980, reported that fluid is produced by three modes of movement within the small intestine: (i) peristalsis, (ii) segmentation, and (iii) oscillation. Peristalsis and segmentation are basically electrical rhythmic movements which causes contraction of the circular muscle layer of the intestinal wall while Peristaltic contractions travel downward via the gut, while segmental contractions are fixed but localized. In contrast, Wobbling causes the luminal contents to move backward in a characteristic oscillatory pattern. Levy et-al., 2016 however reported that Peristalsis parameters like frequency and force of intestinal contractions are influenced by slow waves and action potentials (Levy et-al., 2016).

In 2013, Guyton and Hall reiterated that Peristalsis propels chyme through the small intestine for about 3 to 6 hours with an average speed of 1.0 cm/m. (Guyton and Hall, 2013). Mixed differences or divergence occurs when a portion of small intestine is fully occupied with chyme; thus, local concentric contractions of the intestine occur (Guyton and Hall, 2006). Different from Peristalsis, segmentation which produces mixing of intestinal contents with minor net flow. Thus, continuous division and subdivision of intestinal contents causes segmental contractions., thereby altering the concentration gradient of any substance in the chyme (Macagno and Christensen, 1980).

II. METHODOLOGY

Formulation of governing equations

The following assumptions were made for the solution;

i. The flow is laminar convection.
ii. Permeability is not considered
iii. A steady-state hydro-dynamically incompressible fluid flow is assumed.
iv. The inlet temperature is 303K.
v. The velocity profile is fully developed in the model.
vi. The velocity along the radial direction is assumed to be zero, that is, the velocity along the radial direction is insignificant compared with the axial velocity.
vii. The effect of gravity is ignored.
viii. No slip boundary condition is used on the walls.
ix. Apply a thermal boundary condition of constant heat flux.

Continuity equation

Continuity equation

$$\frac{\partial U_r}{\partial r} + \frac{1}{r}\frac{\partial U_\emptyset}{\partial \emptyset} + \frac{\partial U_x}{\partial x} = 0 \quad (1)$$

$U_x$is the only non-zero velocity component, so

$$U_r = U_\emptyset = 0 \quad (2)$$

Equation 3.1 simplifies to

$$\frac{\partial U_x}{\partial x} = 0 \quad (3)$$

Equation (3) proves independent of the radial component of the tube, which means thin-walled tubes and is the same for all values of x.$U_x U_x = U_x(r)$

$$U_x = U_x(r) \quad (4)$$

momentum equation

Radial:

$$\rho\left(\frac{\partial U_r}{\partial t} + U_r\frac{\partial U_r}{\partial r} + \frac{U_\emptyset}{r}\frac{\partial U_r}{\partial \emptyset} + U_x\frac{\partial U_r}{\partial x} + \frac{{U_\emptyset}^2}{r}\right) = \rho g_r - \frac{\partial P}{\partial r} + \mu\left[\frac{\partial^2 U_r}{\partial r^2} + \frac{1}{r^2}\frac{\partial^2 U_r}{\partial \emptyset^2} + \frac{\partial^2 U_r}{\partial x^2} + \frac{1}{r}\frac{\partial U_r}{\partial r} - \frac{2}{r^2}\frac{\partial U_\emptyset}{\partial \emptyset} - \frac{U_r}{r^2}\right] \quad (5)$$

For non-Newtonian fluids; $\tau_{w=\mu_o}\left(\frac{du}{dr}\right)^n$ where n is the index number

Azimuth direction

$$\rho\left(\frac{\partial U_\emptyset}{\partial t} + U_r\frac{\partial U_\emptyset}{\partial r} + \frac{U_\emptyset}{r}\frac{\partial U_\emptyset}{\partial \emptyset} + U_x\frac{\partial U_\emptyset}{\partial x} + \frac{{U_\emptyset}^2}{r}\right) = \rho g_\emptyset - \frac{\partial P}{\partial \emptyset} + \mu\left[\frac{\partial^2 U_\emptyset}{\partial r^2} + \frac{1}{r^2}\frac{\partial^2 U_\emptyset}{\partial \emptyset^2} + \frac{\partial^2 U_\emptyset}{\partial x^2} + \frac{1}{r}\frac{\partial U_\emptyset}{\partial r} + \frac{2}{r^2}\frac{\partial U_r}{\partial \emptyset} - \frac{U_\emptyset}{r^2}\right] \quad (6)$$

Axial

$$\rho\left(\frac{\partial U_x}{\partial t} + U_r\frac{\partial U_x}{\partial r} + \frac{U_\emptyset}{r}\frac{\partial U_x}{\partial \emptyset} + U_x\frac{\partial U_x}{\partial x}\right) = \rho g_x - \frac{\partial P}{\partial x} + \mu\left[\frac{\partial^2 U_x}{\partial r^2} + \frac{1}{r^2}\frac{\partial^2 U_x}{\partial \emptyset^2} + \frac{\partial^2 U_x}{\partial x^2} + \frac{1}{r}\frac{\partial U_x}{\partial r}\right] \quad (7)$$

Substituting equations (2) and (3) into equations (5) and (6), we get

$$\frac{\partial P}{\partial r} = 0 \quad (8)$$

$$\frac{\partial P}{\partial \emptyset} = 0 \quad (9)$$

From equations (8) and (9)

$$\frac{\partial P}{\partial r} = \frac{\partial P}{\partial \emptyset} = 0 \quad (10)$$

Equation (10) shows that the pressure depends only on the axial direction.

Substituting into equations (2) and (3) and imposing the steady state condition yields

$$\frac{\partial U_x}{\partial t} = 0 \quad (11)$$

$$0 = \rho g_x - \frac{\partial P}{\partial x} + \mu\left[\frac{\partial^2 U_x}{\partial r^2} + \frac{1}{r^2}\frac{\partial^2 U_x}{\partial \emptyset^2} + \frac{\partial^2 U_x}{\partial x^2} + \frac{1}{r}\frac{\partial U_x}{\partial r}\right] \quad (12)$$

rearrange

$$\frac{\partial P}{\partial x} = \rho g_x + \mu\left[\frac{\partial^2 U_x}{\partial r^2} + \frac{1}{r^2}\frac{\partial^2 U_x}{\partial \emptyset^2} + \frac{\partial^2 U_x}{\partial x^2} + \frac{1}{r}\frac{\partial U_x}{\partial r}\right] \quad (13)$$

By applying Eq. (2) and ignore gravitational effects

$$\frac{\partial P}{\partial x} = \mu\left[\frac{\partial^2 U_x}{\partial x^2}\right] \quad (14)$$

Equation (14) is the momentum transfer equation of the model.

energy equation

The energy transfer equation for the steady state flow is;

$$k\frac{\partial^2 T}{\partial r^2}+\frac{k}{r^2}\frac{\partial^2 T}{\partial \emptyset^2}+\frac{\partial^2 T}{\partial x^2}+\frac{k}{r}\frac{\partial T}{\partial r}+\emptyset_{(i)}= \quad \rho C_p\left[U_r\frac{\partial T}{\partial r}+U_\emptyset\frac{\partial T}{\partial \emptyset}+U_x\frac{\partial T}{\partial x}\right] \tag{15}$$

Substituting Equation (2) into the viscous dissipation term, the equation simplifies to:$\emptyset_{(i)}$

$$k\frac{\partial^2 T}{\partial r^2}+\frac{k}{r^2}\frac{\partial^2 T}{\partial \emptyset^2}+\frac{\partial^2 T}{\partial x^2}+\frac{k}{r}\frac{\partial T}{\partial r}=\rho C_p\left[U_r\frac{\partial T}{\partial r}+U_\emptyset\frac{\partial T}{\partial \emptyset}+U_x\frac{\partial T}{\partial x}\right] \tag{16}$$

Since is the only non-zero velocity component, the equation applies. (2) and dividing by k will result in:U_x

$$\frac{\partial^2 T}{\partial x^2}+\frac{1}{r}\frac{\partial T}{\partial r}=\frac{\rho C_p}{k}\left[U_x\frac{\partial T}{\partial x}\right] \tag{17}$$

and$$\alpha=\frac{k}{\rho C_p} \tag{18}$$

Equation (12) simplifies to

$$\frac{\partial^2 T}{\partial x^2}=\frac{U_x}{\alpha}\frac{\partial T}{\partial x} \tag{19}$$

Equation (19) is the energy transfer equation for the flow in the tube.

A. Small intestine model diagram

A numerical model consists of three basic steps: data pre-processing, solution procedure, and data post processing. In the pre-processing step, a sketch of the simulation platform is done with

Inventor 2017, establish mesh division of the model in Design Modeller, and fix the initial conditions and boundary conditions. Next, implement a suitable numerical scheme to solve the governing equations of the model. Finally, in a post-processing step, the data needs to be properly analyzed and visualized to ensure proper discussion of the results.

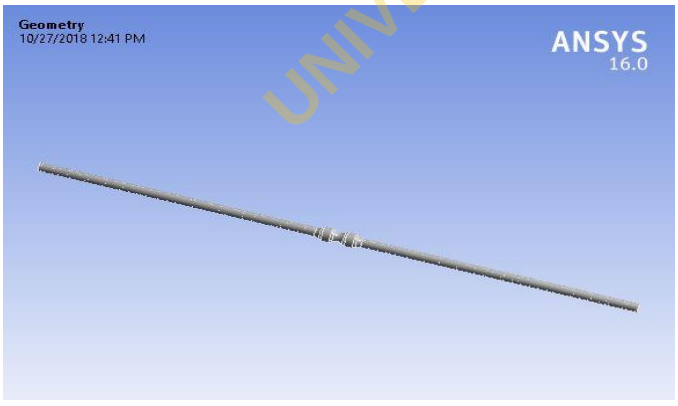

Fig. 1: Simulated gut

B. CFD Solver Settings.

Numerical simulations are performed by solving 3-D Navier-Stokes and continuity equations. Numerical studies were performed using the solver ANSYS FLUENT 16.0 (Academic Edition), which discretized the governing equations using Finite Element Method. In this process, the computational platform is discretized by a grid of a range of element sizes, and the governing equations are then solved.

After importing and checking the mesh for a given problem, complete the following setup:

i. Numerical solver choices are Pressure Based, Absolute Velocity Formulation, 3D Axisymmetric and Stable.
ii. Select the appropriate physical model: viscous laminar flow model, with optional viscous heating and energy equations.
iii. Chyme and production fluid; inputs for Ogi, Soya, and Sobo attributes are shown in Table 4.1
iv. In the fluid domain, the corresponding fluid to be checked is selected from the drop-down list of input fluids.
v. Enter the boundary conditions for the inlet and walls. Since the flow is velocity-driven, an inlet velocity of 0.005m/s with a gauge pressure of 100Pa was first selected, followed by other velocities for continuous fluid selection. Additionally, a constant heat flux is applied to the wall.
vi. Set up the convergence monitor with a continuity of 1.0e-07, a convergence criterion for the X, Z, and Y coordinates, and an energy residual of 1.0e-08.
vii. Set the solution method: the pressure-velocity coupling is processed by the SIMPLE scheme. Under Spatial Discretization, select Gradient, 2nd order Upwind based on least squares elements for the momentum and energy equations.
viii. The number of iterations was set to 1000 before running the calculation. Iteratively solves the discretized conservation equations using the built-in Gauss Siedel method. The solution converges at 5000 iterations.

For post processing of the solver, velocity, pressure and temperature contours were generated. In addition, lines were created on the geometry to serve as planes of interest, and the mean values of the fluid properties were evaluated along each line, as shown in Fig. 1.

Calculated values of average velocity, pressure change, fluid velocity, fluid pressure, fluid temperature, Reynolds number and shear rate, and wall shear stress were evaluated.

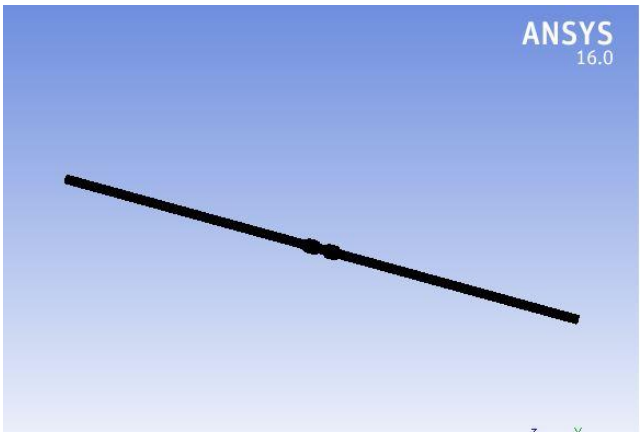

Fig. 2: Mesh generation domain.

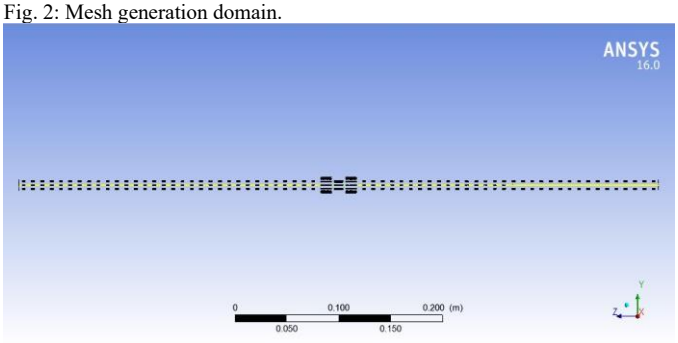

Fig. 3: Geometrically imaginary line/plane

Table 1 shows the hydrodynamics of chyme and the resulting liquid supplements; Ogi, Soymilk and Sobo noodles. The table shows that Ogi is more viscous and denser than the other two fluids, while sobo has the smallest density and viscosity values.

Table 1: Thermophysical properties of the fluids considered in this study.

Table 1: Thermophysical properties of the fluids considered in this study.

Fluid	Density(kg/m 3)	Viscosity (Pa·s)	Specific heat capacity (J/(kg·K))	Thermal conductivity (W/(m•K))
Chyme	1000	1	4180	0.600
Pap (Augie)	1024	1.095	1840	0.536
Soy milk (soy)	920	0.95	3970	0.501
Hibiscus sabdariffa roselle (Sobo)	800	0.316	2470	0.491

III. RESULTS AND DISCUSSION

The most common boundaries in restricted fluid flow problems are walls. This is also commonly referred to as boundary condition with no-slip, with appropriate conditions for wall velocity component and normal component that can be set to zero. When a condition of flows occurs in parallel layers with no breaks within the layers and it tends to occur at lower velocities then Laminar or streamlined flow is identified. Figs. 4 and 7 are velocity contours for non-Newtonian fluid flow in the intestine, with no slip boundary condition and zero velocity. Fig. 4 shows the velocity profile along the transverse tube section and the velocity streamlines of the simulated intestine. Figs. 5 to 7 show various flows along the axial position for different inlet velocities.

As shown in Figs. 8 to 10, there is propulsive motion of the intestine pushing the fluids towards distal ends of the intestine, an increase in velocity can be observed and characterized by a propulsive wave-like propagation to a point of 1.1 m for various inlet velocities and maintaining Even speed up to the pulsating part of the model intestine, where the speed suddenly drops and then increases towards the end. Fig. 11 shows that the four fluids behave similarly, they have the same hydrodynamic flow, there is a peristaltic motion of relaxation and contraction of the intestine, and they have same velocity variation along axial position. There may also be a peristaltic rush because the infection diarrhea causes motility and rapid peristalsis called peristaltic rush.

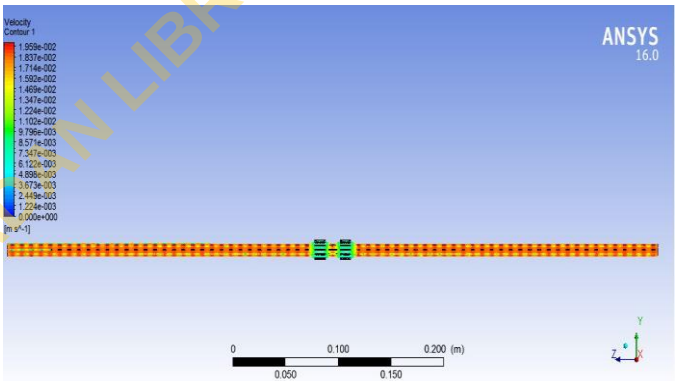

Fig. 4: Velocity distribution along the length of simulated intestine

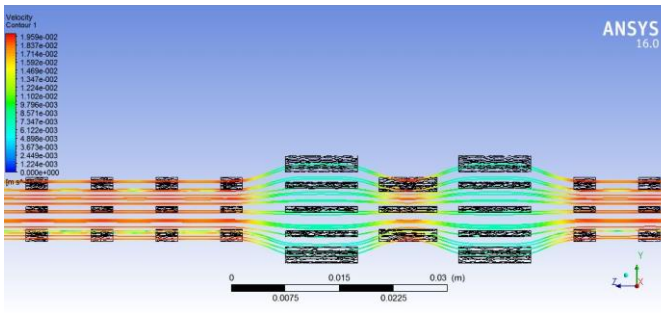

Fig. 5: Velocity Contour of simulated part of the gut

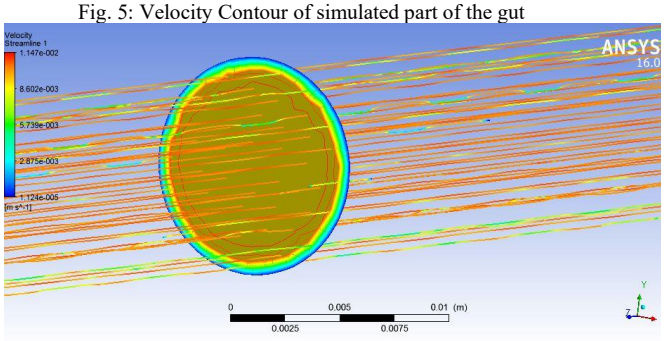

Fig. 6: Velocity streamlines of the pipe cross-section at 0.8m of the simulated gut

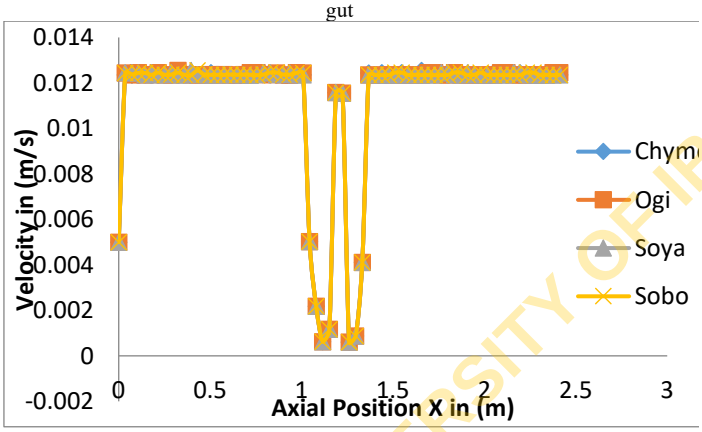

Fig. 7: Flow velocity as function of axial position along the domain centreline for inlet velocity of 0.005 m/s.

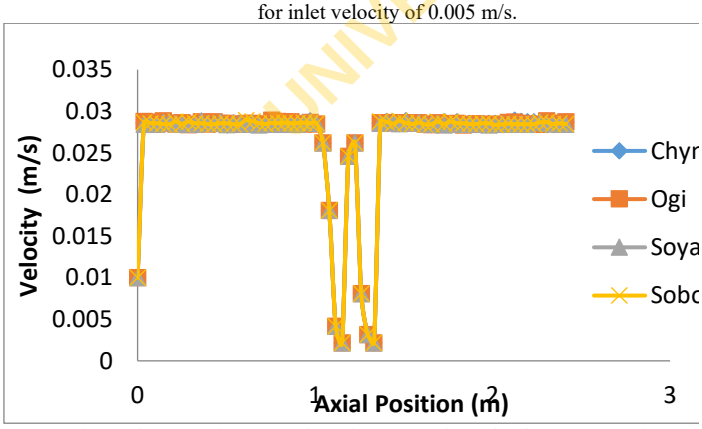

Fig. 8: Flow velocity as function of axial position along the domain centreline for an inlet velocity of 0.01 m/s

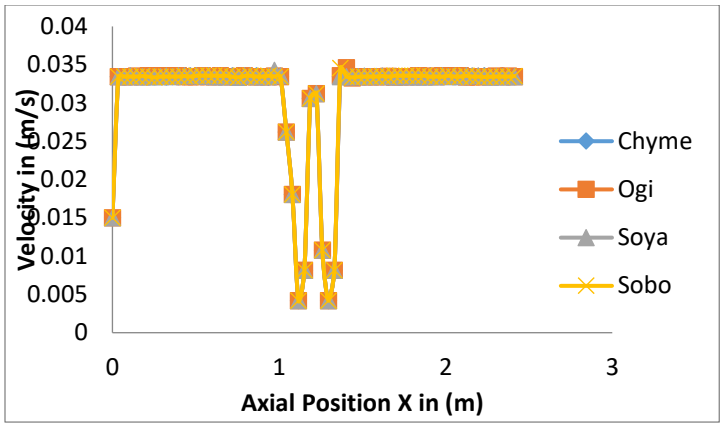

Fig. 9: Flow velocity as function of axial position along the domain centreline for an inlet velocity of 0.015 m/s.

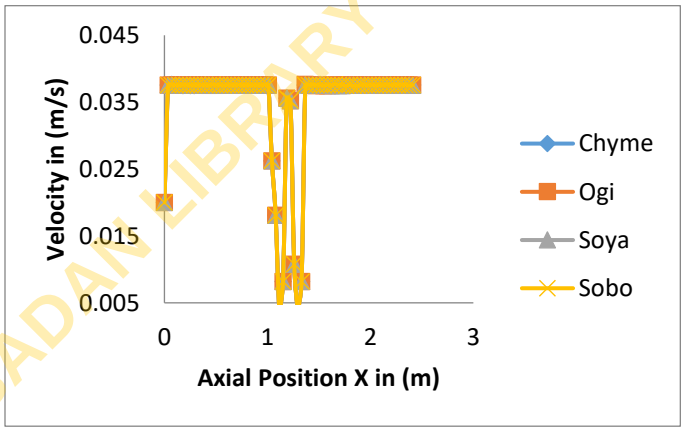

Fig. 10: Flow velocity as function of axial position along the domain centreline for an inlet velocity of 0.02 m/s

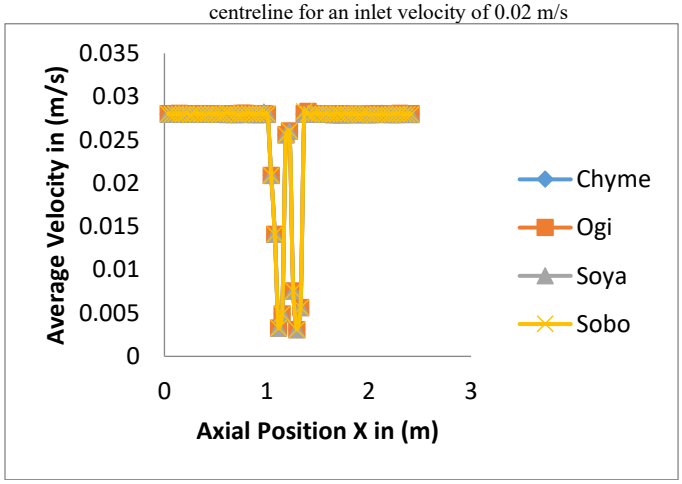

Fig. 11: Variation of mean velocity with axial position for different fluids

IV. CONCLUSION AND RECOMENDATION

A Conclusion

At the end of the investigation, the under listed conclusions were made;

i. The density and viscosity of the produced fluid are (Ogi=1024 kg/m^3, soymilk=920 kg/m^3 and sobo=800 kg/m^3) and (ogi=1.095 Pa.s soymilk= 0.95 Pa.s and

sobo=0.316 Pa .s), respectively. The resulting liquids; ogi, soymilk and soba noodles were found to be pseudoplastic.

ii. The governing equations were developed and applied and found to be suitable for this study.

iii. Autodesk INVENTOR 2017 was found to be a useful tool for modeling the gut.

iv. ANSYS 16.0 was found to be good software for simulation, especially for numerical analysis of the current work.

B Recommendations

The production of next-generation healthy foods capable of delivering nutrients in the gastrointestinal passage requires thorough understanding of material science, medical physics, physical chemistry, and biophysics, coupled with adequate knowledge of how food and food materials are processed and the resultant effects on structures of the food and hence the underlined recommendations;

i. In-vitro digestion models be developed in order to have detailed understanding of kinetics involved in food breakdown in relation to hydrodynamic and mechanical contraction forces present in vivo.

ii. Further research be done toward exploration of the relationship between food texture, microstructure, chemical properties and digestive properties such as disintegration rate and gastric emptying rate since kinetics and regulatory mechanisms vary for different types of food, such as meat, baked goods, vegetables and nuts.

iii. In addition, studies should also be directed towards understanding the significant influence of the rheological properties of gastric juice, intragastric fluid movement and hydrodynamics on food digestion.

Nomenclature

h	Heat transfer coefficient	J/K
k	Thermal Conductivity	W/m·K
Nu	Nusselt number	
m	mass	kg
P	pressure	N/m^2
q	spread heat	Joule (J)
r	The radius of the simulated intestine rice	
Re	Reynolds number	
V	Average speed	m/s
T	temperature	^0C
u_r	Velocity along the radial direction multiple sclerosis	
$U_\emptyset$	Velocity along the azimuth direction multiple sclerosis	
Axial speed multiple sclerosis		
ρ	density	kg/m3
μ	dynamic viscosity	pa.s
C_p	specific heat capacity	J/kg
Dh	hydraulic diameter rice	
Uavg	average speed	

REFERENCES

1.Abrahamsson B., Pal A., Sjöberg M., Carlsson M., Laurell E. and Brasseur JG (2013), Fiction In Vitro and Numerical Analysis of Shear-Induced Drug Release released tablet in fed stomach, Pharmaceutical Research, 22(8), 1215–26.

2.Akbar, NS and Nadeem, S. (2014). Simulation of chyme motility in the small intestine For coupling pressurized fluids. Mechanics, 49:325-334.

3.Akbar, N. S, Nadeem, S, Hayat, T., and Hendi, AA Heat and Mass Transfer 48, 451 (2013). Journal of Computational and Theoretical Nanoscience, Vol. 10, 2491–2499,

4.Astrup A, Dyerberg J, Elwood P, Hermansen K, Hu KB. 2011. Effects of reduced intake Saturated fats prevent cardiovascular disease: Evidence 2010, Am J Clin Nutrit 93:684-8.

5.Arrieta, J., Cartwright, JHE, Gouillart, E., Piro, N., Piro, O., Tuval, I. (2015). Geometric Stomach mixing, gastric peristalsis, and geometric phase. A 10(7):

6.Blackburn NA, Holgate AM and Read NW (1984) Meal hyperglycemia in humans by reducing the contact area of the small intestine British Journal of Nutrition, 52(2), 197-204.

7.Buettner A., Beer A. and Hannig C. and Settles M. (2015) Swallowing Observations Applied telescopic and real-time magnetic techniques for processing Resonance Imaging the result of post-nasal aroma stimulation, Chemical Senses, 26, 1211–1219.

8.Boyer J. and Liu RH (2014) Apple phytochemicals and their health benefits, Nutrition *Magazine,*3, 5.

9.Carragher P. and LJ Crane, "Heat transfer on continuously stretched surfaces", Zeitschrift frAngewandte Mathematik and Mechanik62, 647-654 (2015).

10.Coulson JM and Richardson JF (1998) Chemical Engineering Volume 1: Fluid Flow, Heat and Mass Transfer, Oxford: Butterworth-Heinemann.

11.Cotran, Seta Y, Kusai A, Ikeda M, Nishimura K. 2015. A Unique Dosage Form to Evaluate Mechanical destructive forces in the gastrointestinal tract. International Journal of Pharmacy 208:61-70.

12.I.K Adegun, O.O. Alabi, S.E. Ibitoye, P.O. Omoniyi, T.S. Ogedengbe, (2020). Numerical investigation of thermo-physical properties of non-newtonian fliud in a modelled intestine, Journal of Bioresources and Bioproducts 5 (2020) 211–221